10. Charged-Particle Lunar Environment Experiment

Brian J. O'Brien [a]† *and David L. Reasoner* [b]

Purpose of the Experiment

The primary scientific objective of the charged-particle lunar environment experiment (CPLEE) is to measure the fluxes of charged particles (electrons and ions) with energies ranging from 50 to 50 000 eV that bombard the lunar surface. The following list illustrates the wide variety of phenomena that may be responsible for these particles:

(1) Relatively stable plasma population in the magnetospheric tail including the so-called plasma sheet and neutral sheet (ref. 10–1)

(2) Transient particle fluxes in the magnetospheric tail resulting from such phenomena as geomagnetic substorms and particle-acceleration mechanisms similar to those that produce auroras (ref. 10–2)

(3) Plasma in the transition region between the magnetospheric tail and the shock front

(4) The solar wind, and particles resulting from the interaction between the solar wind and the lunar surface (refs. 10–3 and 10–4)

(5) Solar cosmic rays, those particles thrown into interplanetary space by solar-flare eruptions

(6) Photoelectrons at the lunar surface produced by the interaction of solar photons with the lunar-surface material

(7) "Artificial events"; for example, particles produced by the impact of the lunar module (LM)

[a] University of Sydney.
[b] Rice University.
† Principal investigator.

Thus, in one sense the Moon serves as a satellite to carry the CPLEE instrument through various regions of space, and in another sense the CPLEE is a detector of phenomena resulting from the interaction of radiation with the lunar surface.

Summary of Observations

In conjunction with the preceding list of scientific objectives, the following preliminary observations have been noted:

(1) Detection of stable, low-energy photoelectron fluxes at the lunar surface

(2) Observation of plasma clouds produced by the impact of the Apollo 14 LM ascent stage

(3) Observations of rapidly fluctuating, low-energy (50 to 200 eV) electrons in the magnetosheath and magnetospheric tail

(4) Detection of fluxes of medium-energy electrons, with durations of a few minutes to some tens of minutes, deep within the magnetospheric tail

(5) Observation of electron spectra in the magnetospheric tail remarkably similar to electron spectra observed above terrestrial auroras

(6) Observation of rapid time variations (10 sec) in solar-wind fluxes observed in interplanetary space

Theoretical Basis

The objectives of the CPLEE are to measure the proton and electron fluxes at the lunar surface and to study their energy, angular distribu-

tions, and time variations. The results of these measurements will provide information on a variety of particle phenomena, important both in themselves and for their relevance to lunar-surface properties.

A category of radiation exists that may periodically envelop the Apollo lunar-surface experiments package (ALSEP) at the times of the full Moon, when it is in the magnetospheric tail of the Earth, which is swept downstream like a comet tail by the solar wind. It has been speculated (ref. 10–2) that the electrons and protons that cause auroras when they plunge into the terrestrial atmosphere are accelerated in the magnetospheric tail. Indeed, it has been shown (ref. 10–5) that the ultimate source of auroral particles is the Sun and furthermore that an almost-continuous replenishment of the magnetospheric-particle population is necessary to sustain the observed auroral fluxes (ref. 10–6). The mechanisms that accelerate these particles to auroral energies are not understood, and simultaneous observations near the Earth and near the Moon are essential for detailed study of their general characteristics and morphology.

The solar wind may occasionally strike the surface of the Moon. The wind is caused by the expansion into interplanetary space of the very hot outer envelope of the Sun. The stream apparently carries energy and perturbations toward the Earth-Moon system; consequently, the solar wind may be the source of energy that leads to such terrestrial phenomena as auroras and Van Allen radiation. For this study, the Moon would serve as an excellent stable observation post in space.

However, apparently the pure interplanetary solar wind does not always hit the lunar surface (ref. 10–3). Because the solar wind is supersonic and because the Moon is sufficiently large to prove an obstacle to the flow of the wind, it is possible that, at times, there is a standing shock front. To date, the only such phenomenon observed is caused by the terrestrial magnetic field, which hollows out a cavity in the solar wind. The detailed physical processes that occur at such shock fronts are not understood fully, and they are of considerable fundamental interest in plasma research. If, occasionally, such a shock front exists near the Moon, the CPLEE will observe the disordered (or thermalized) fluxes of electrons and protons that share energy on the downstream side of the shock. Apparently, the "shadowing" of the solar wind by the lunar surface, causing a plasma "void" on the dark side, is the most frequently occurring situation (ref. 10–3).

The instrument can also measure the lower energy solar cosmic rays occasionally produced in solar eruptions or flares. To observe these low-energy particles, the experimental packages must be placed beyond the reach of the modifying effects of an atmosphere and a magnetic field such as exists on Earth. The Moon is an excellent platform for such studies because both the atmosphere and magnetic field are so relatively negligible.

The sunlit lunar surface may be a veritable sea of low-energy photoelectrons generated by solar photons striking the surface. If such electrons are present, the CPLEE, with the capability to detect electrons with energies down to 40 eV, will be in an excellent position to study them. Studies of any such photoelectron layer are important in deducing surface properties related to photoemission and in gaining indirect information about lunar-surface electric fields.

Observations of the charged-particle environment of the Moon are of interest also, not merely for its own sake but because such particles affect the lunar environment. They may cause luminescence or coloration effects on the lunar surface. The charged particles may also sweep away a large proportion of the lunar atmosphere. Furthermore, they constitute a very important proportion of the electrical environment, and they may, for example, nullify electrostatic effects that would otherwise occur on the lunar surface.

Equipment

Description of the Instrument

The CPLEE consists of a box supported by four legs. The box contains two similar physical charged-particle analyzers, two different programable high-voltage supplies, twelve 20-bit accumulators, and appropriate conditioning and shifting circuitry. The total weight on Earth is approxi-

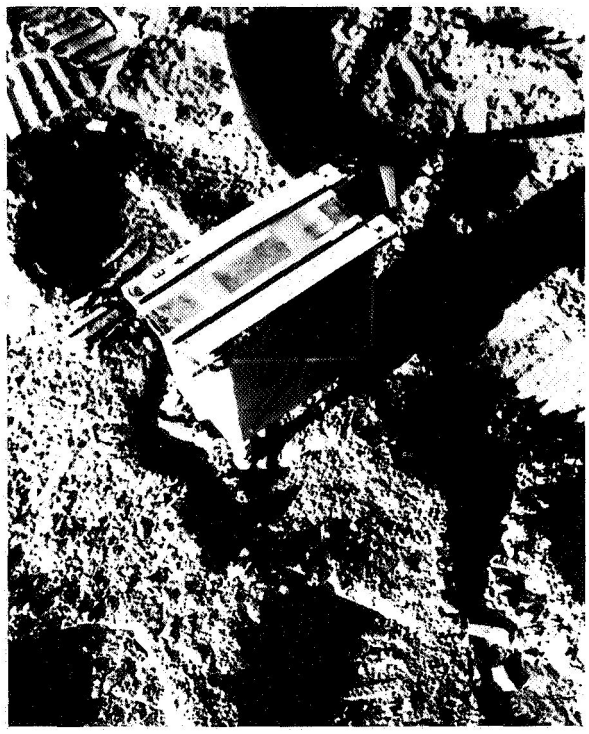

FIGURE 10–1.—The CPLEE deployed on the lunar surface. Photograph illustrates the absence of dust contamination and the east-west alinement of the CPLEE.

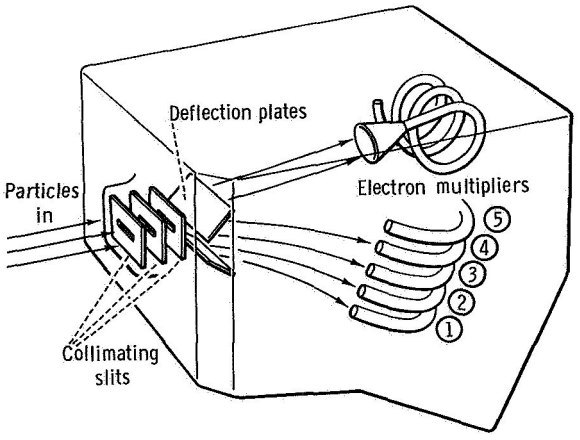

FIGURE 10–2.—Schematic sketch of the CPLEE physical particle analyzer, showing the deflection plates and channel electron-multiplier stack.

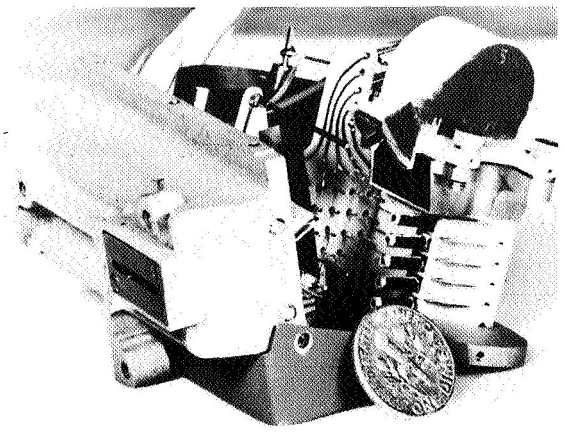

FIGURE 10–3.—The CPLEE physical particle analyzer.

mately 2.7 kg (6 lb), and normal power dissipation is 3.0 W rising to approximately 6 W when the lunar-night survival heater is on. The CPLEE is shown deployed on the lunar surface in figure 10–1.

Each physical analyzer contains five C-shaped channel electron multipliers with a nominal aperture of 1 mm each and one helical channel electron multiplier with a nominal aperture of 8 mm. These are shown schematically in figure 10–2 and an actual analyzer is shown in figure 10–3.

The channel electron multiplier is a hollow glass tube, the inside surface of which, when bombarded by charged particles, ultraviolet light, etc., is an emitter of secondary electrons. In the CPLEE, the aperture of each electron multiplier is operated nominally at ground potential (actually at 16 V), while a voltage of 2800 or 3200 V (selected by ground command) is placed on the other (i.e., anode) end. Thus, if an incident particle enters the aperture and secondary electrons are produced, these are accelerated and hit the walls to generate more secondary electrons, so that a multiplication to an order of 10^7 is achieved by the time the pulse arrives at the anode. After conditioning, pulses from each electron multiplier are accumulated in a register for later readout as described in the following paragraphs.

As shown in figure 10–2, incident particles enter an analyzer through a series of slits and then pass between two deflection plates across which a voltage can be applied. Thus, at a given deflection voltage, the five small-aperture electron multipliers make a five-point measurement of the energy spectrum of charged particles of a given polarity (e.g., electrons), while, simultaneously, the large-aperture electron multiplier makes a

single wideband measurement of particles with the opposite polarity (e.g., protons). The advantages of simultaneously measuring particles of opposite polarity and of simultaneous multiple-spectral samples are considerable in studies of rapidly varying particle fluxes.

The CPLEE particle analyzer is quite similar to the switched proton electron Channeltron spectrometer (SPECS) (ref. 10–6) and, in fact, the SPECS instrument was the prototype of the CPLEE anlyzer. The capability of the SPECS, and thus of the basic particle analyzer of the CPLEE, was demonstrated by a series of sounding-rocket flights in 1967 and 1968 (refs. 10–1 and 10–5) and on the Rice University-Office of Naval Research satellite Aurora 1 (refs. 10–7 and 10–8.

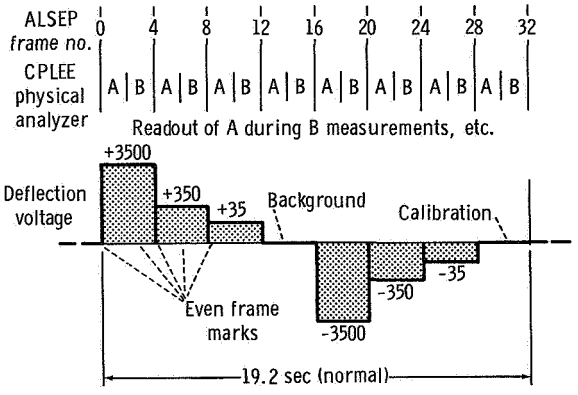

FIGURE 10–4.—Deflection-voltage stepping sequence of the CPLEE in the automatic mode. At the +0 step, the background level is measured and at the −0 step, a test oscillator is injected into the accumulators.

In the CPLEE, the deflection-plate voltage, in the normal mode, is stepped in the sequence shown in figure 10–4. As a consequence, the energy passbands shown in figure 10–5 are sampled. Although data acquired by the six sensors are not transmitted simultaneously, the six sensors are connected to six accumulators for exactly the same time (viz, 1.2 sec) and the contents transferred to shift registers for later sequential transmission.

Two analyzers, *A* and *B*, point in the directions shown in figure 10–6. The same deflection voltage is applied to each analyzer simultaneously, with counts from 1.2-sec accumulation time of analyzer *A* being transmitted while counts from analyzer *B* are accumulating. Thus, each voltage is normally on for 2.4 sec with the result that the total cycle time is 19.2 sec (fig. 10–4), when allowance is made for two sample times when the deflection voltage is zero. On one of those two occasions, counts are accumulated as usual to measure background or contaminating radiation. On the other occasion, a pulse generator of about 375 kHz is connected to the accumulators to verify operation.

The command link with the ALSEP provides a variety of options for CPLEE operation. Aside from the usual power commands common to all

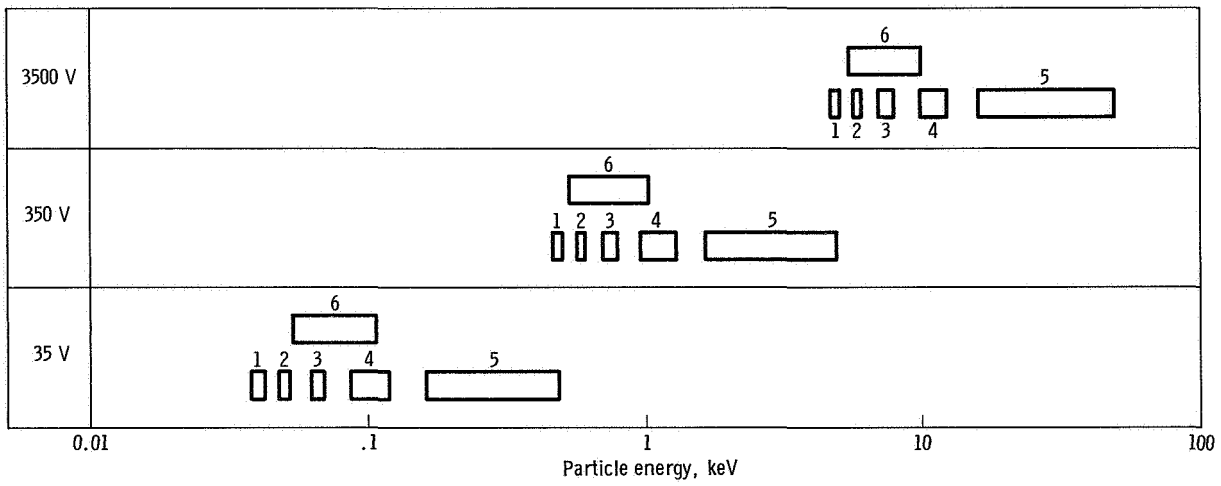

FIGURE 10–5.—Rectangular equivalent energy passbands of the CPLEE.

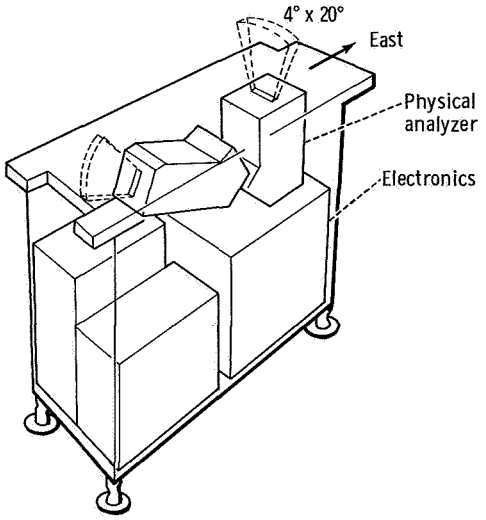

FIGURE 10–6.—Sketch of the CPLEE, showing the fields of view and the look directions of the physical analyzers.

ALSEP experiments, three commands are provided that allow the normal automatic stepping sequence to be modified. The sequence can be stopped and then the deflection plate supply can be manually stepped to any one of the eight possible levels. This is done to study a particular phenomenon (e.g., low-energy electrons) with higher time resolution (2.4 sec). A second set of commands allows the electron-multiplier high-voltage supply to be set at either 2800 or 3200 V. The higher voltage is used in the event the electron-multiplier gains decrease during lunar operations. A third pair of commands allows the normal thermal-control mode to be bypassed in the event of failure of the thermostat, thus offering manual control of the heaters.

The CPLEE apertures are covered with a dust cover to avoid contamination during deployment and, particularly, during LM ascent (ref. 10–9). The dust cover was made doubly useful because a ^{63}Ni radioactive source was placed on the underside over each aperture. Thus, the sensors were proof calibrated on the Moon, and the data compared with measurements made in the same way with the same system when the unit was last calibrated on Earth.

Calibration

Calibration of the CPLEE was extensive and will be described briefly in this report. The major portion of the calibration was performed with an electron gun that fired a large, uniform beam of electrons of adjustable energy levels, monoenergetic to approximately 2 percent. Under the control of a computer, the instrument was tilted at various angles to the beam. The computer stored the count rates of each channel at each angle and electron energy level as well as the beam current measured by use of a Faraday cup. The absolute geometric factors were then computed from the several million accrued measurements. In addition, the ^{63}Ni sources were used as broadband near-isotopic electron sources for standard calibrations.

In practice, the exact passbands were derived, rather than the rectangular equivalent passbands of figure 10–5. However, the finer details, together with information gained from measuring susceptibility to ultraviolet light and to scattered electrons, can be shown to be negligible for this preliminary study.

Deployment

The CPLEE was deployed with no difficulty at approximately 18:00 G.m.t. on February 5, 1971. Leveling to within 2.5° and east-west alinement to within ±2° were to be accomplished with a bubble level and a Sun compass, respectively.

It has since been determined by a careful study of the lunar photographs and a comparison of predicted and actual solar ultraviolet response profiles that the experiment is 1.7° off level, tipped to the east, and 1° away from a perfect east-west alinement. This error is well within the preflight specifications. Furthermore, the photograph (fig. 10–1) shows no visible dust accretion on the exterior surfaces.

Operation of the Experiment

The CPLEE was first commanded on at 19:00 G.m.t., February 5, during the first period of extravehicular activity for a brief functional test of 5-min duration. All data and housekeeping channels were active, and the instrument began

operation in the proper initial modes (i.e., automatic sequencer, on; electron-multiplier voltage increase, off; and automatic thermal control, on).

A complete instrument checkout procedure was initiated at 04:00 and continued until 06:10 G.m.t., February 6. During this period, data from the dust-cover beta sources were accumulated and compared with prelaunch calibrations. A partial comparison is shown in a following section of this report. Also during this period, all command functions of the CPLEE were exercised except the forced heater mode and dust-cover removal commands. The instrument responded perfectly to all commands. After the checkout procedure, the CPLEE was commanded to the standby mode to await LM ascent.

Following LM ascent, the CPLEE was commanded on at 19:10 G.m.t. and the dust cover was successfully removed at 19:30 G.m.t., February 6. The CPLEE immediately began returning data on charged-particle fluxes in the magnetosphere.

The instrument temperatures were carefully and continuously monitored for 45 days after deployment. It was found that the temperature range was nominal, with the internal electronics temperature ranging from 58° C at lunar noon to —24° C during lunar night. The total lunar eclipse of February 10 offered an excellent opportunity to determine various thermal parameters and to test the capability of the CPLEE to survive extreme thermal shocks. A plot of the physical-analyzer temperature during the eclipse is shown in figure 10–7. The maximum thermal shock occurred after umbra exit, with a temperature change rate of 25° C/hr. Also from this figure, it is possible to derive a thermal time constant of approximately 1.9 hr. The CPLEE suffered no ill effects from this period of rapid temperature changes.

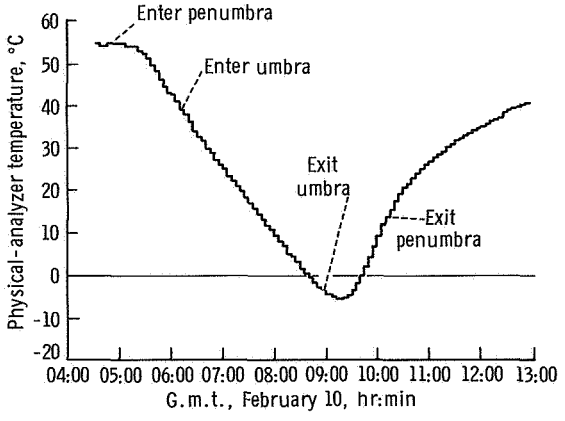

FIGURE 10–7.—Temperature profile of CPLEE during the total lunar eclipse of February 10.

The command capability of the CPLEE was used extensively during the 45-day real-time support period to optimize scientific return from the instrument. Alternate 1-hr periods of manual operation at the —35-V step and automatic operation have been used to concentrate on rapid temporal variations in low-energy electrons. Similarly, alternate periods of 350-V manual and automatic operation have been used to focus on rapid changes in magnetopause ions and the solar wind. In fact, the manual operation capability and the attendant 2.4-sec sampling interval made possible the detection of phenomena that would have been impossible to detect otherwise because of sampling problems and aliasing. Most of the decisions concerning operational modes were based on viewing the real-time data stream.

To date, the CPLEE has operated continuously with all high voltages on except for one brief period of approximately 15 sec when it was commanded to standby, and then back to on, to restore automatic thermal control at the termination of the first lunar night. No evidence of high-voltage discharge or corona has been observed.

Results

The following paragraphs are a detailed discussion of the scientific phenomena recorded by the CPLEE and listed in the "Summary of Observations." In many cases, these phenomena are quite distinct, and hence each phenomenon, complete with data, discussion, and conclusions, is presented in following portions of this section.

Beta-Source Tests

Abbreviated results of three separate beta-source tests (with the CPLEE subjected to exci-

TABLE 10–I. *Beta-Source Tests of the CPLEE*

Calibration and date	*Readout on channel—*					
	1	*2*	*3*	*4*	*5*	*6*
Analyzer A:						
Precalibration, Oct. 24, 1969	8.7	22.2	38.8	80.7	165.7	1280.5
Postcalibration, Jan. 20, 1970	8.2	18.9	38.5	86.6	205.7	1323.0
Postdeployment, Feb. 6, 1971	10.68	20.5	39.6	82.4	195.9	1259.0
Analyzer B:						
Precalibration, Oct. 24, 1969	5.8	12.7	19.8	43.6	113.1	777.7
Postcalibration, Jan. 20, 1970	4.5	9.1	14.6	34.8	96.6	577.9
Postdeployment, Feb. 6, 1971	7.68	12.0	17.8	35.4	90.0	763.8

tation by the ^{63}Ni beta sources mounted under the dust cover) are presented in table 10–I. The tests were conducted before the complete laboratory calibration, immediately after the laboratory calibration, and after lunar deployment. These tests span an interval of approximately 15 months.

The counting rates tabulated are for deflection voltages of −3500 V for channels 1 to 5 and 3500 V for channel 6, when the channels were sensitive to electrons with energies between 5 and 50 keV. Variations in analyzer *A* are not more than 30 percent, with 4 to 6 percent being typical. In analyzer *B*, there was a general trend of gain loss between the precalibration and postcalibration tests of approximately 20 percent, but there was a partial recovery between the postcalibration test and the postdeployment test. This effect is attributed to the well-known characteristic of temporary electron-multiplier fatigue resulting from exposure to high fluxes (e.g., during the calibration) and later recovery. This phenomenon has been documented (ref. 10–10). These beta-source tests show that no major changes occurred in the electron-multiplier characteristics between calibration and deployment, and they verified the operation of CPLEE. The small variations in gain observed are to be expected and are tolerable.

Photoelectron Fluxes

One of the most stable and persistent features in the CPLEE data is the presence of low-energy electrons when the lunar surface, in the vicinity of the ALSEP, is illuminated by the Sun. It was possible early in the mission to prove that these fluxes were of photoelectric origin, by observing the disappearance of the fluxes during the total lunar eclipse of February 10. The counting rates of channel 6 at 35-V deflection (sensitive to electrons with 50 eV $< E <$ 150 eV) of both analyzers *A* and *B* before, during, and after the eclipse are shown in figures 10–8 and 10–9. The

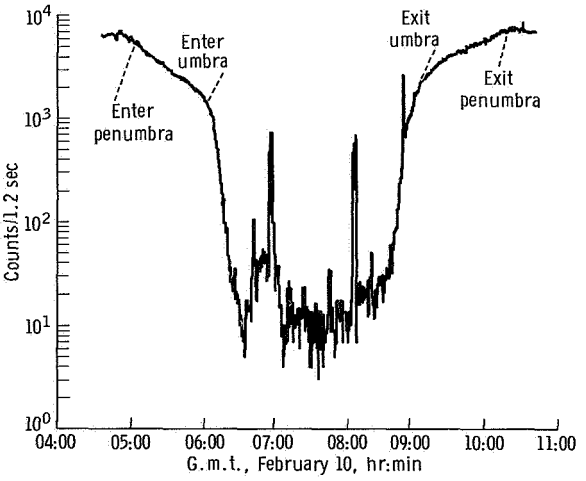

FIGURE 10–8.—Counting rate of channel 6 of analyzer *A* at 35 V, measuring electrons with energies between 50 and 150 eV for the period including the lunar eclipse.

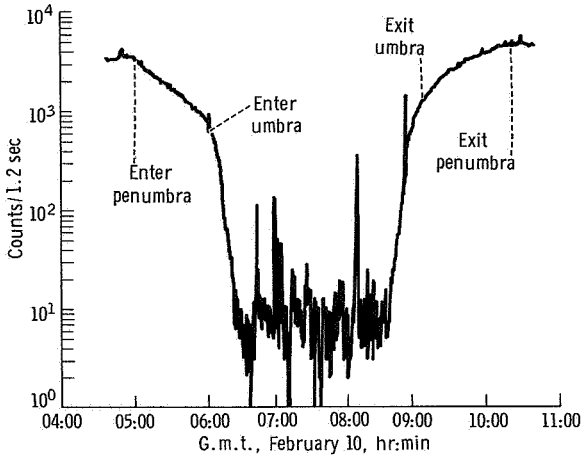

FIGURE 10–9.—Counting rate of channel 6 of analyzer *B* at 35 V, measuring electrons with energies between 50 and 150 eV for the period including the lunar eclipse.

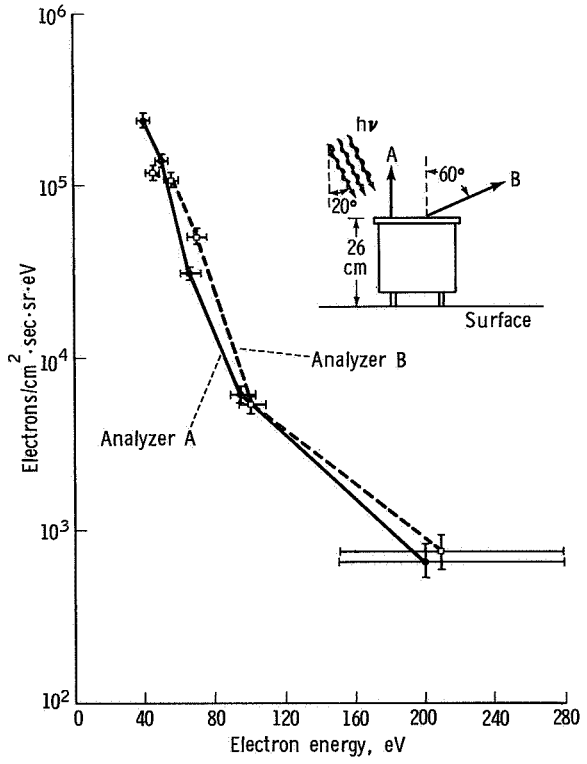

FIGURE 10–10.—Energy spectrum of photoelectrons with energies between 40 and 200 eV. The sketch on the figure shows the geometry of CPLEE relative to the lunar surface and to the direction of solar radiation.

flux is seen to correlate exactly with the presence of illumination; and, during the eclipse, sporadic bursts of electrons, presumably of magnetospheric origin, occur with flux levels that are normally undetectable because of the masking effect of the photoelectrons.

The energy spectrum of these photoelectrons, obtained from channels 1 to 5 at −35 V at a period just before eclipse onset, is shown in figure 10–10 for both analyzers. As would be expected, the spectrum is quite steep, as the CPLEE was observing essentially a high-energy and possible nonthermal tail of an electron distribution with an average energy of approximately 2 eV. In fact, the high-energy tail that was measured was almost certainly nonthermal, because the spectrum between 40 and 100 eV can be represented by an equation of the form

$$j(E) = j_0 \exp\left[\frac{-(E-40)}{14}\right]$$

where $j(E)$ is electron flux in units of electrons/cm² · sec · sr · eV and j_0 is the flux at $E = 40$ eV. Clearly, this does not agree with a simple maxwellian distribution at low energies with $kT \approx 2$ eV. Two possible explanations for this discrepancy exist: (1) Some process is acting to accelerate part of the photoelectron gas; (2) the CPLEE itself is at a positive potential with respect to the surrounding lunar-surface average potential. The second explanation is entirely possible in view of the facts that the CPLEE is well insulated from the lunar surface by fiber-glass legs and that the photoemissive properties of the CPLEE and of the lunar surface are almost certainly different. It is hoped that this question will be resolved with detailed studies of these photoelectron fluxes, especially during periods of terminator crossings and the eclipse.

It should also be noted that, although in one sense the photoelectron fluxes are a contaminant obscuring weak fluxes of magnetospheric origin (fig. 10–8), they are valuable not only because they furnish information of solar-radiation/lunar-surface interactions but also because they furnish a stable "calibration source" for monitoring long-term changes in electron multiplier operating characteristics. To put it another way, the photo-

electrons offer a continuing "beta-source" test for monitoring the performance of the instrument.

At certain angles between the Sun line and the analyzer look directions, preflight ultraviolet-rejection tests showed enhanced counting rates because of photoelectrons produced inside the analyzers. The enhanced counts reported here must be due to photoelectrons from the lunar surface because both analyzers *A* and *B* recorded comparable fluxes. It would be impossible for a single-point ultraviolet source (e.g., the Sun) to produce such similar counting rates in both analyzers.

LM Impact Event

On February 7, the Apollo LM ascent stage impacted the lunar surface 66 km west of the CPLEE. The terminal mass and velocity were 2303 kg and 1.68 km/sec, respectively, resulting in an impact energy of 3.25×10^{11} J (sec. 6). The LM contained approximately 180 kg of volatile propellants, primarily dimethylhydrazine fuel and nitrogen tetroxide oxidizer. For the purpose of reference and orientation, figure 10–11 is a lunar map showing the location of the impact point relative to the Apollo 12 and 14 ALSEP sites.

The counting rates of channel 6 of analyzer *A* (measuring ions with energies of 50 to 150 eV/unit charge) and channel 3 of the same analyzer (measuring negative particles with energies of 61 to 68 eV) are shown in figure 10–12 from 00:44:53 to 00:48:55 G.m.t. on February 7.

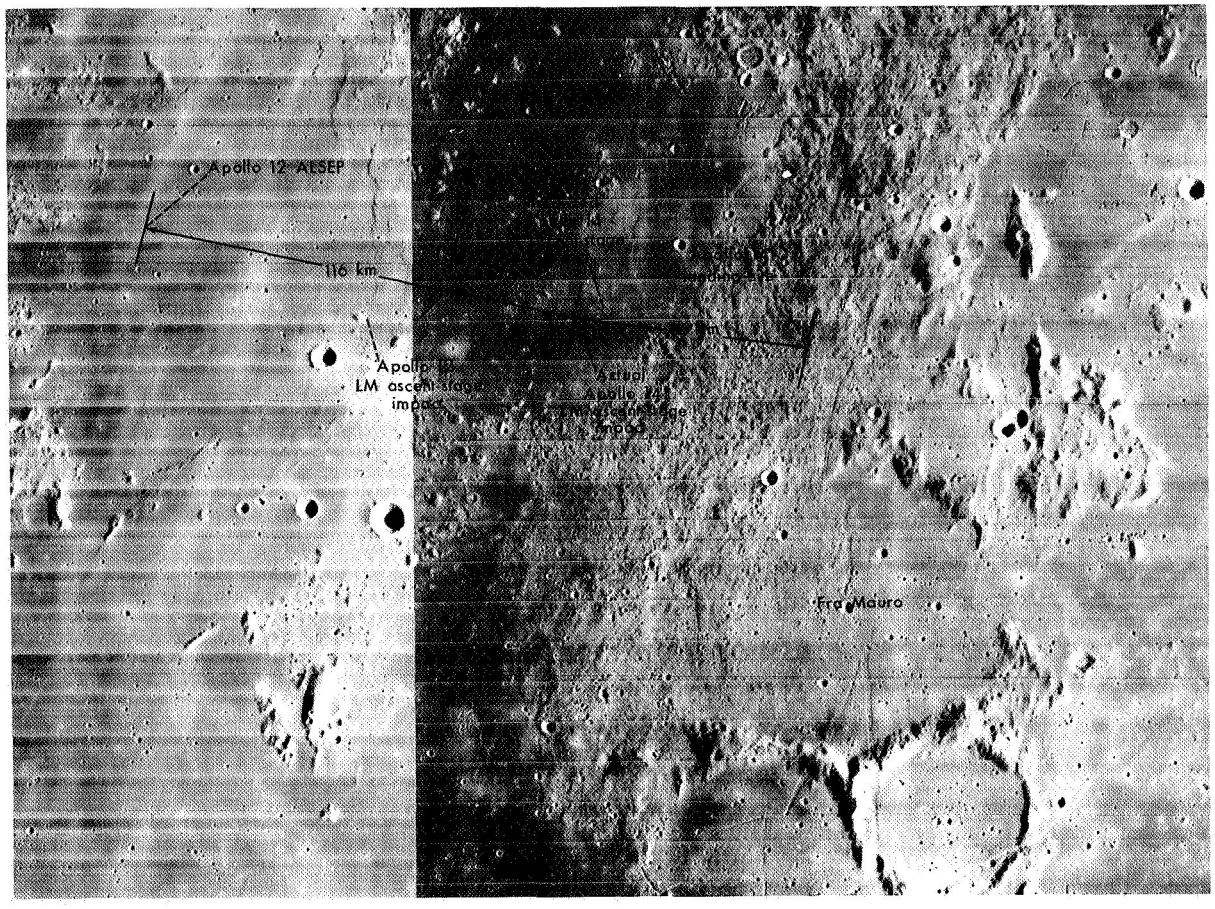

FIGURE 10–11.—Lunar map showing the locations of the CPLEE and of the Apollo 14 LM ascent-stage impact point.

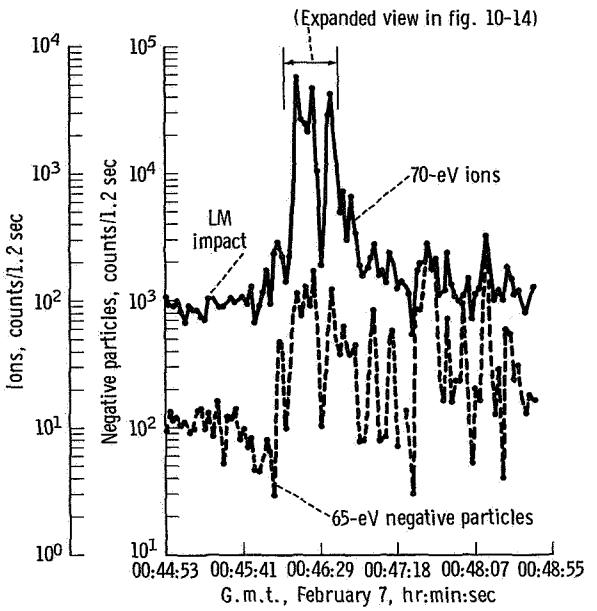

FIGURE 10–12.—Counting rates of channels 3 and 6 of analyzer *A* at −35 V, measuring 65-eV negative particles and 70-eV ions, respectively, showing the particle fluxes resulting from the LM impact.

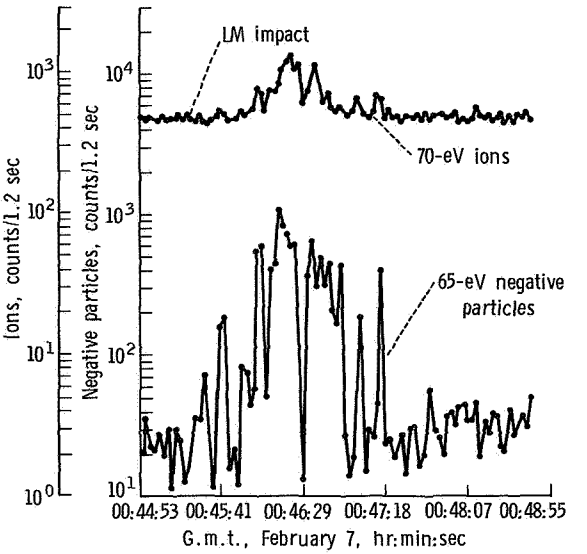

FIGURE 10–13.—Counting rates of channels 3 and 6 of analyzer *B* at −35 V, measuring 65-eV negative particles and 70-eV ions, respectively, showing the particle fluxes resulting from LM impact.

As can be seen from figure 10–12, the counting rates before and during the LM impact were reasonably constant and, by all indications, were due to the ambient population of low-energy electrons and ions that are present whenever the lunar surface, in the vicinity of the CPLEE, is illuminated. (This conclusion is supported by the observation that these ambient fluxes disappeared entirely during the total lunar eclipse (figs. 10–8 and 10–9) that occurred a few days later on February 10.) The counting rates increased by a factor of about 4 approximately 40 sec after LM impact and then reverted to ambient levels for a few seconds. However, 48 sec after LM impact, the ion electron counting rates increased very rapidly by a factor of up to 40 as the plasma cloud enveloped the CPLEE. A second plasma cloud passed the CPLEE a few seconds later, as shown by the second large peak. On the assumption that the plasma clouds traveled essentially in a linear path between the impact point and the CPLEE, the average velocity calculated was 1.0 km/sec; and the horizontal dimensions were 14 and 7 km for the first and second clouds, respectively.

The same data for analyzer *B* oriented 60° from the vertical toward the lunar west (i.e., toward the impact point) are shown in figure 10–13. By comparing figures 10–12 and 10–13, it can be noted that the flux enhancements were essentially simultaneous in the two directions, but that the positive-ion flux measured by analyzer *A* was five times higher than the flux measured by analyzer *B*. On the other hand, the negative-particle flux measured by analyzer *A* was only one-third as great as the negative-particle flux measured by analyzer *B*.

The detailed characteristics of the plasma clouds are shown in figure 10–14, which is an expanded-time-scale plot of the negative-particle fluxes in five energy ranges and the ion flux in a single energy range measured by analyzer *A*. The plot shows clearly that the negative-particle enhancement was confined to energies less than 100 eV, because the 200-eV flux was essentially constant throughout the event. Furthermore, the spectrum of negative particles during the enhancement is quite different from the background electron spectrum. This point is illustrated further in figure 10–15, which shows the negative-particle spectra for 00:42:33 G.m.t. (before the LM impact) and

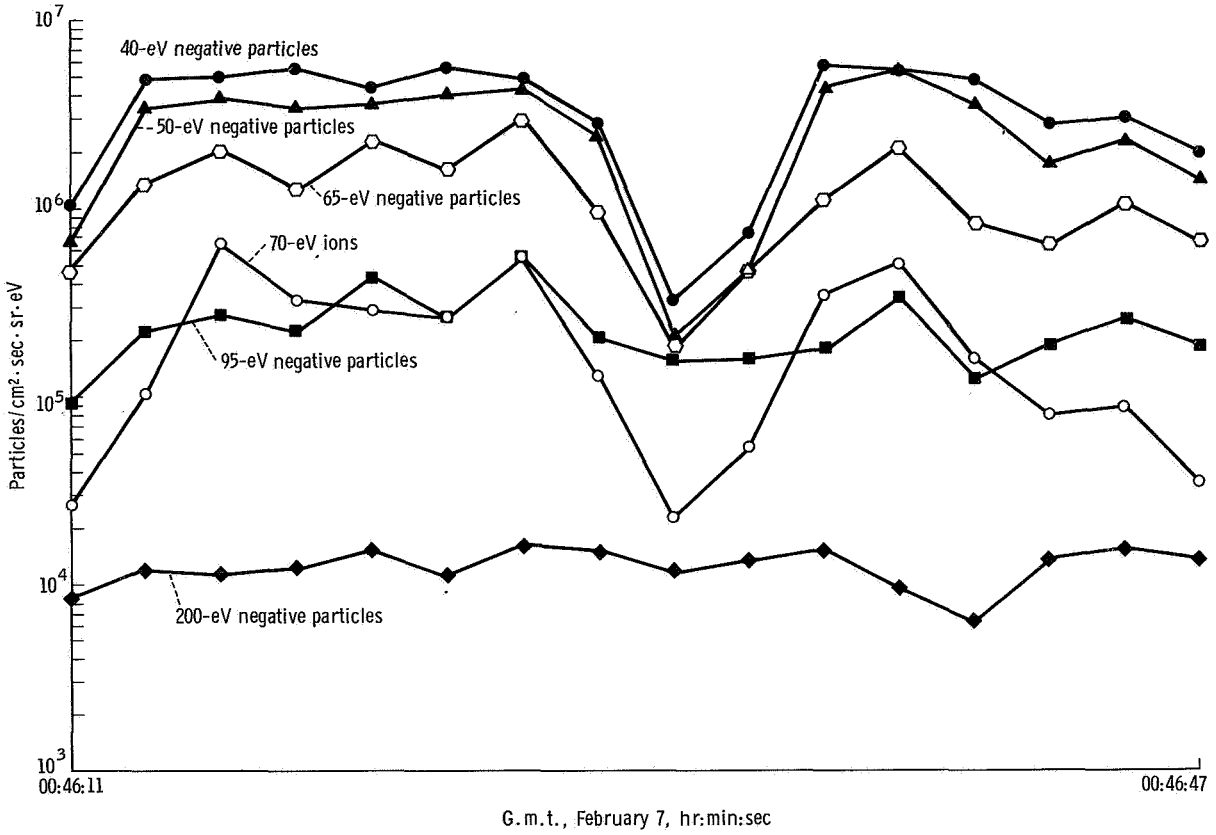

FIGURE 10–14.—Expanded view of the data of figure 10–12, showing details of the two prominent peaks. The fluxes are computed from five negative-particle energy ranges and a single positive-ion energy range.

00:46:19 G.m.t., February 7 (at the peak of the first plasma cloud).

It might well be questioned whether the flux enhancements at 48 and 67 sec after LM impact were actually initiated by the event. In the period of approximately 2 days following the impact event, several rapid enhancements in the low-energy electron fluxes (by a factor of up to 50) were observed. However, these other enhancements were not correlated with positive-ion-flux increase; and, in fact, the event referred to is the only such example of perfectly correlated positive- and negative-particle enhancements recorded to date. In addition, careful monitoring before the LM impact revealed that the fluxes were relatively stable, constant to within a factor of 2 over periods of a few minutes. This observation lends credence to the belief that this was a valid case of cause and effect.

Further confidence in the interpretation that the flux enhancements were artificially impact produced rather than of natural origin is gained by noting that, although no such plasma clouds have previously been detected resulting from impact events, positive-ion clouds have been detected by the Apollo 12 suprathermal ion detector experiment. These positive-ion clouds were interpreted as resulting from the Apollo 13 and 14 SIVB impacts.[1]

[1] J. W. Freeman, Jr.; H. K. Hills; and M. A. Fenner: Some Results From the Apollo 12 Suprathermal Ion Detector. Proc. Apollo 12 Lunar Sci. Conf. (Houston), Jan. 11–14, 1971. To be published in Geochim. Cosmochim. Acta.

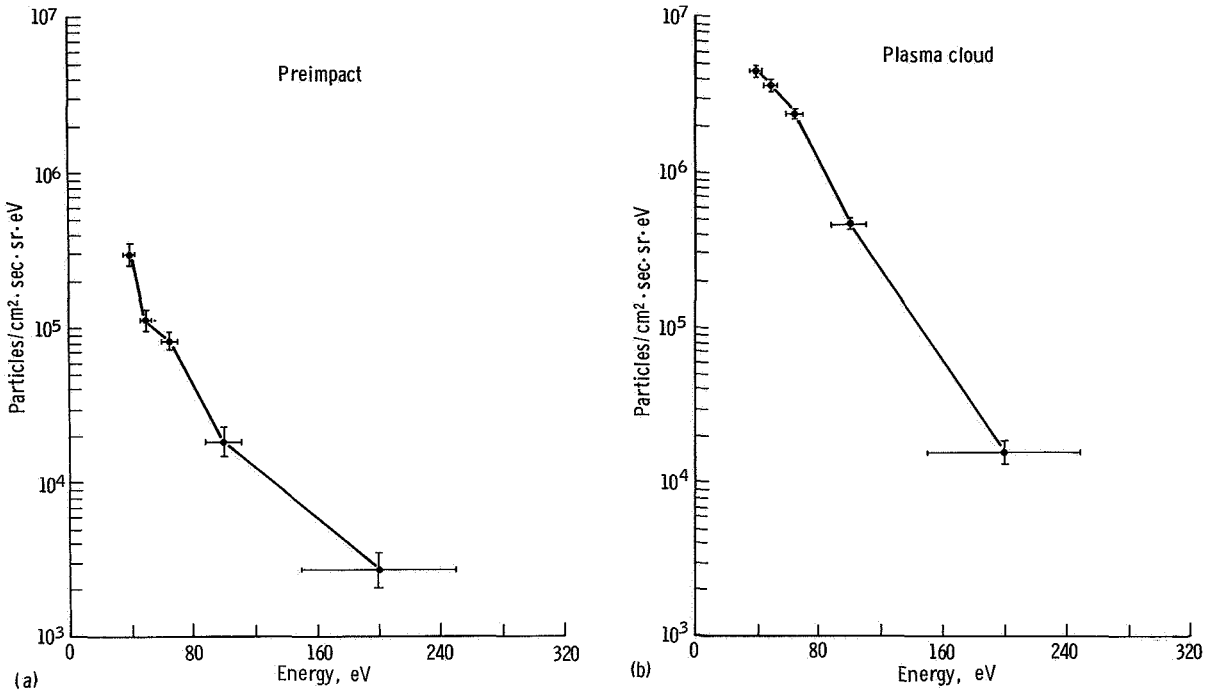

FIGURE 10–15.—Negative-particle spectra measured by analyzer *A* for two periods. (a) The spectrum a few minutes before LM impact. (b) The spectrum at the height of the first large peak shown in figure 10–12.

Some detailed parameters calculated from the flux enhancements are discussed next. An average cloud velocity of 1 km/sec has been previously noted, and it is of interest to compare this with particle velocities in the cloud. Some assumptions must, of course, be made as to the ion species present. Considering that the most likely source of ions was the LM propellants, an average ion mass of 25 is estimated. If it is assumed that the negative particles detected were electrons and that the positive particles had an average mass of 25, this assumption yields velocities ($E = 50$ eV) of 4000 km/sec and 20 km/sec, respectively. The charged-particle energy densities based upon the ions actually measured are calculated to be 5.6×10^{-10} erg/cm^3, assuming the ions were protons, and 28.0×10^{-10} erg/cm^3, assuming an average ion mass of 25. These are lower limits, because positive ions were measured in only a single energy range, and an overall ion-energy spectrum is required to make a more exact calculation. The magnetic-field energy density at the lunar surface, based on Apollo 12 lunar-surface-magnetometer measurements (ref. 10–11) of a steady 35γ field is 50×10^{-10} erg/cm^3; hence, the particle energy density appears to be at least comparable to and possibly dominant over the magnetic-field energy density. This conclusion, however, may be modified by the Apollo 14 lunar portable magnetometer observations of lunar-surface fields of 40 to 100 gammas at two distinct sites (sec. 13). It should also be noted that the solar-wind energy density is 80×10^{-10} erg/cm^3.

Therefore, the conclusion can be made that the LM impact resulted in the production of two annular plasma clouds that contained negative particles and ions with energies up to 100 eV. The particles traveled across the lunar surface with a velocity of approximately 1 km/sec. No speculation has been made as to the mechanisms responsible for production of these clouds, but the simultaneous arrival of both positive- and negative-charge species is impossible to reconcile with a simple model of photodissociation and ionization and subsequent acceleration by a static electric field.

The fact that the electron and ionic components were detected simultaneously offers a unique problem; because, if one assumes that the particles were energized at the instant of impact, a mechanism must be found that is able to hold the cloud together, in view of the fact that measured ion velocities exceed the cloud velocity by an order of magnitude. This fact in itself argues against ambipolar diffusion. Processes such as charge exchange, scattering, and wave-particle interactions can also be rejected by appealing to considerations based on the size of the clouds (10 km). The only remaining possibility is magnetic confinement, or a process whereby the local magnetic field confines the particles in circular orbits. There is, however, a criticism of the hypothesis that magnetic confinement can explain the observation. The cyclotron radii of the particles must be no greater than the dimension of the plasma cloud. The cyclotron radius of a 50-eV mass-25 ion in a 100γ magnetic field is 50 km, or a factor of approximately 3 to 6 times larger than the inferred cloud dimensions.

It thus appears that a simple model of the particles being energized at the instant of impact is untenable not in itself, but because a mechanism to contain the plasma after energization is not readily evident and, in fact, may not exist. The alternate conclusion is that the impact produced expanding gas clouds, and the particles in these gas clouds were then ionized by any one of several means (e.g., photoionization) and subsequently accelerated by a continuously or erratically active acceleration mechanism. The solar-magnetospheric (SM) coordinates of the CPLEE at the time of impact were $Y_{SM}=34R_E$, $Z_{SM}=21R_E$, and solar elevation angle $=30°$, where R_E is Earth radius. (The solar-magnetospheric coordinate system is based on the Earth-Sun line (X-axis) and the magnetic dipole axis of the Earth. The Z-axis is perpendicular to the Earth-Sun line and in the plane formed by the Earth-Sun line and the Earth magnetic dipole axis; the Y-axis completes the right-handed coordinate system.) Hence, it is highly likely that the solar wind had direct access to the lunar surface at this time. Noting the energy densities of the solar wind and the plasma cloud particles, the solar wind is energetically capable of being the energy source. Whether any such mechanism can work is unknown at this time, although calculations have indicated that the solar wind can interact with a neutral gas through means other than simple particle-particle collisions (ref. 10–12).

In summary, the impact-event data apparently indicate a situation in which the gas cloud, solar wind, and local magnetic field are all interacting, offering a unique and fascinating problem in plasma physics.

Low-Energy Electron Fluctuations

In addition to the stable low-energy photoelectron population that the CPLEE records whenever the lunar surface in the vicinity of the CPLEE is illuminated, the CPLEE also observes rapidly varying fluxes of low-energy electrons of magnetospheric origin, with intensities large enough to be detected above the photoelectron background. Examples of these fluxes are shown in figure 10–16, wherein the counting rates of channel 3 (65-eV electrons) and channel 5 (200-eV electrons) are plotted for a brief time segment. At approximately 21:20 G.m.t., February 7, the solar magnetospheric coordinates of the CPLEE were $Y_{SM} = 24R_E$ and $Z_{SM} = 14R_E$, locating the instrument within the magnetospheric tail near the boundary. The instrument was in the manual mode, and hence the individual measurements are 2.4 sec apart. The flux enhancements range up to a factor of 10 above the background level on time scales on the order of a few seconds.

At first glance, the enhancements in the two energy ranges appear to be well correlated, but a closer examination of the figure reveals temporal dispersions in the enhancements. To illustrate this point more clearly, the data for the period 21:20:07 to 21:20:41 G.m.t. have been plotted in a special manner in figure 10–17: a log-log plot of the counting rates in the two energy channels was made with the higher energy channel on the vertical axis and the lower energy channel on the horizontal axis. Each pair of count rates from the two channels is represented by a single point, and a vector is drawn between successive points in the direction of increasing time. On this type of plot, if the enhancements are perfectly correlated, all vectors will lie along a constant slope, the magnitude of which is a function of the relative enhancements. A burst where the higher energy electrons

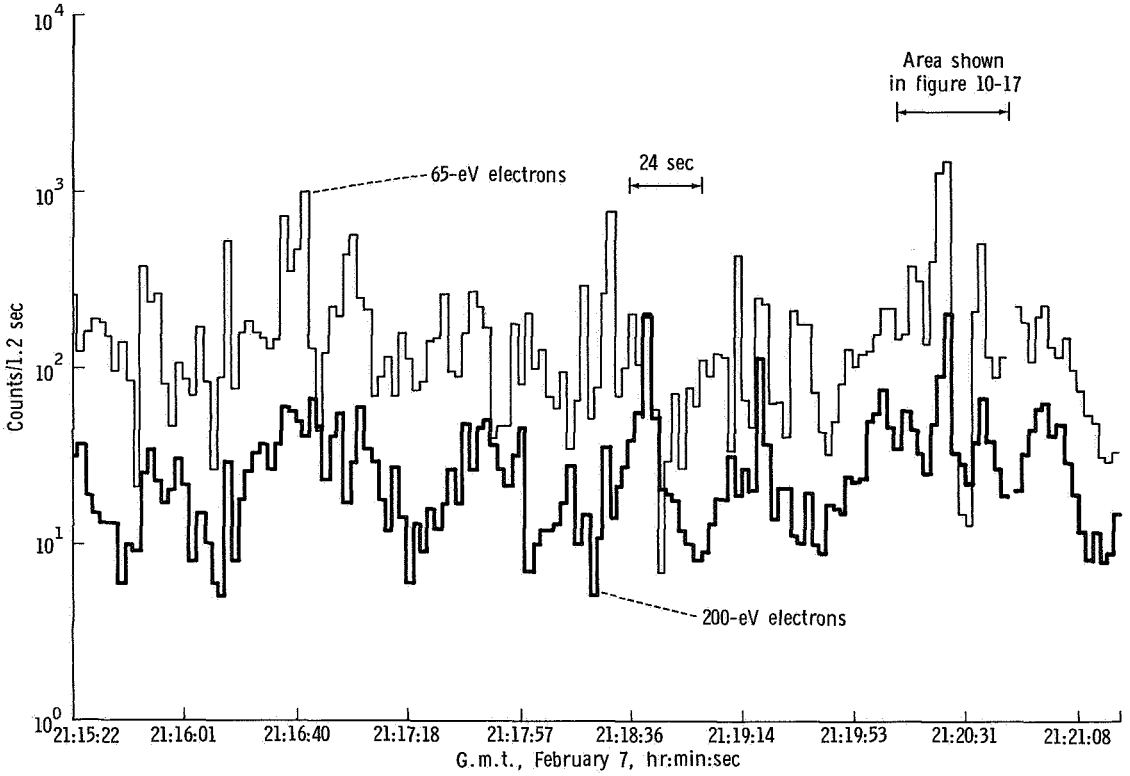

FIGURE 10–16.—Example of rapid variations in magnetospheric low-energy electron fluxes. The data are from channels 3 and 5 of analyzer *A* at −35 V, measuring 65- and 200-eV electrons, respectively.

lead the lower energy electrons will result in an open figure with the vectors rotating clockwise; likewise, if the higher energy electrons lag the lower energy electrons, the vectors will rotate counterclockwise. An examination of figure 10–17 shows that, in general, for the longest vectors, the constant-slope rule is followed; but that on smaller scales (e.g., points 1 to 5 and 9 to 12), considerable deviations from the constant-slope rule exist. For these events, the vectors rotate clockwise, indicating that the higher energy electrons lead the lower energy electrons.

Although plots such as these are indicative in nature, they do show the general character of the enhancements and suggest that low-energy electrons are being accelerated or modulated by processes relatively near the Moon. An approximate estimate of the distance can be obtained by considering the velocity difference at the two energies and the dispersion times in the enhancements (0 sec to approximately 2 sec), resulting in a maximum distance of some 20 000 km, or $3R_E$. An extensive cross-correlation analysis will be necessary to refine these calculations, but the preliminary studies indicate the presence of local (with reference to the Moon) processes capable of modulating or accelerating low-energy electron fluxes.

Medium-Energy Electron Event

At approximately 18:30 G.m.t. on March 10, distinct enhancements in medium-energy (approximately 1-keV) electron fluxes were observed in both analyzers *A* and *B*. The enhancements ranged up to an order of magnitude above background and lasted from a few minutes up to 2 hr; the entire event lasted approximately 4 hr. The gross temporal features of these enhancements are shown in figure 10–18 by giving the counting rate of channel 6 at 350 V (500- to 1500-eV electrons) from 18:30 to 23:00 G.m.t. The data gaps at 19:30 and 21:30 G.m.t. were due to the fact

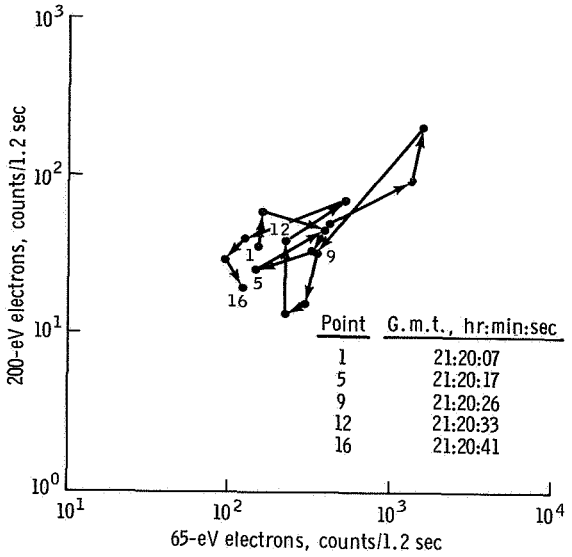

FIGURE 10–17.—Electron correlation analysis of the CPLEE analyzer *A*. A detailed study of a portion of the data of figure 10–16. The counting rate of channel 5 (200-eV electrons) is plotted against the counting rate of channel 3 (65-eV electrons) on a log-log scale. Perfect temporal simultaneity would result in all vectors lying parallel to a line of constant slope. The marked deviations from this rule should be noted.

that the CPLEE was in the manual mode at −35 V at these times, and the data gap at 21:00 was due to a temporary shutdown of the data display system at the NASA Manned Spacecraft Center.

It is seen from the figure that the event is characterized by erratic, relatively short-duration flux enhancements between 18:30 and 21:00 G.m.t.; by a period of stable high fluxes between 21:10 and 22:00 G.m.t.; and by a return to erratic enhancements between 22:00 and 23:00 G.m.t. The magnetic-activity index K_p was 3 or less on March 10, and there were no enhancements in the solar X-ray flux. Thus, this event apparently is characteristic of the quiet-time magnetosphere, and the electrons are truly magnetospheric in origin.

On the basis of the particle measurements alone, it is difficult to resolve the question of whether the enhancements are of a spatial or temporal nature; that is, whether the effects of the CPLEE moving in and out of stable spatial region or regions of flux enhancements are being recorded or whether a large-scale temporal event is being recorded. The cyclotron radius of a 1-keV

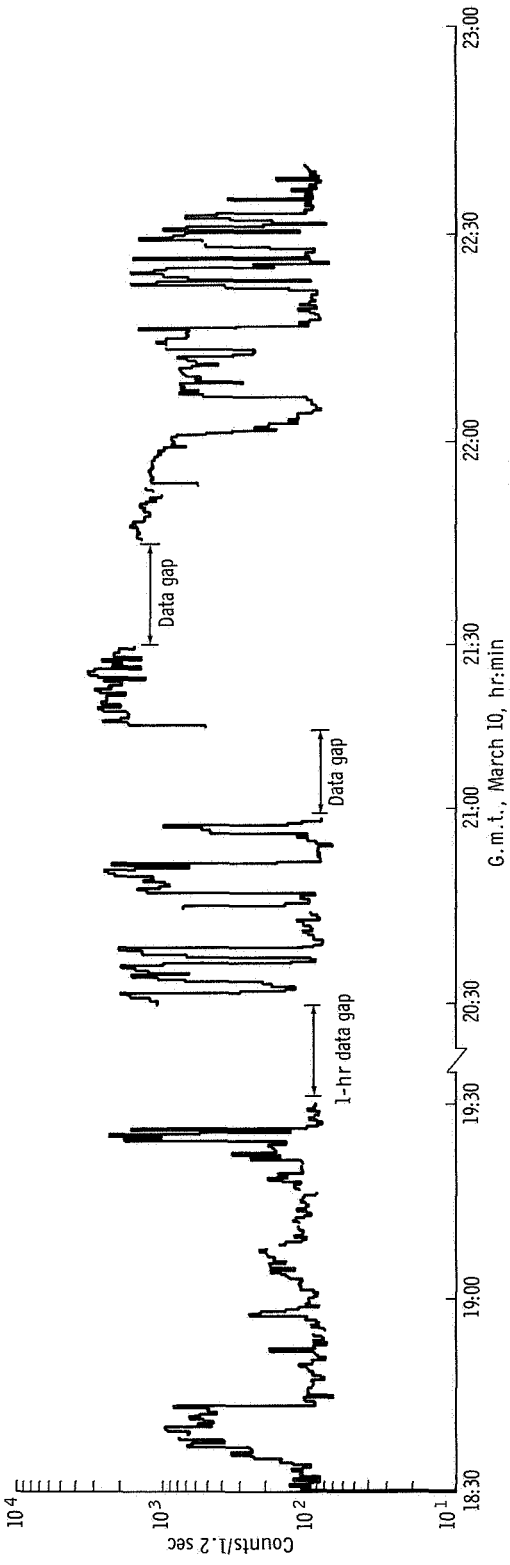

FIGURE 10–18.—Medium-energy (approximately 1-keV) electron event of March 10. The counting rate of channel 6 of analyzer *A* at 350 V indicates the gross features of the event.

electron in a 10γ field, typical of the magnetic tail at lunar distances (ref. 10–13), is 10.6 km, and the Moon moves a distance of approximately 20 km between data samples.

The path of the CPLEE in the solar-magnetospheric Y-Z plane is shown in figure 10–19. Of particular interest is the fact that the event was seen only during the period when Z_{SM} was near the maximum positive excursion of $6R_E$. This is highly suggestive, though certainly not conclusive proof, that the CPLEE was sampling a stable spatial structure located at $Z_{SM} = 6R_E$ and $Y_{SM} = 11R_E$ to $13R_E$. Further indirect evidence is that there is no extended trailing edge in the events. The leading and trailing edges appear equally sharp.

The electron energy spectrum—averaged over the time from 21:45 to 22:00 G.m.t., March 10, the period of the most stable fluxes (fig. 10–18)—is shown in figure 10–20. The photoelectron continuum is the dominant contribution between 40 and 100 eV, but a suggestion of a peak exists in the spectrum of these magnetospheric electrons at 600 eV. Also shown is an upper limit to the background equivalent flux from all other sources at 500 eV, showing the order-of-magnitude enhancement seen in the event. The integrated flux for electrons with energies between 500 and 2000 eV is 4.5×10^6 electrons/cm^2 · sec · sr.

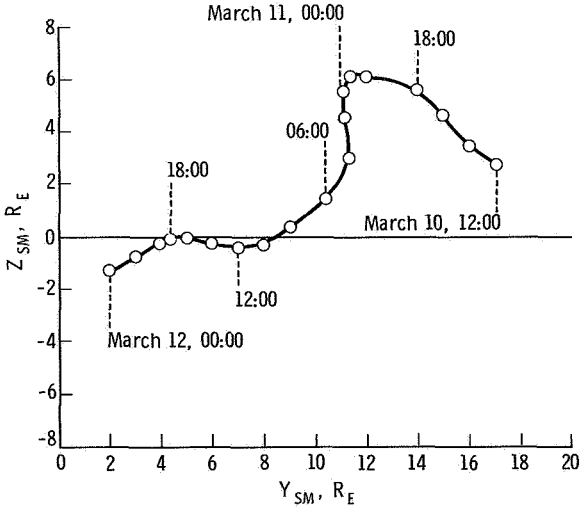

FIGURE 10–19.—Track of the CPLEE in the Y_{SM}-Z_{SM} plane for March 10 to March 12, including the period of the electron event shown in figure 10–18.

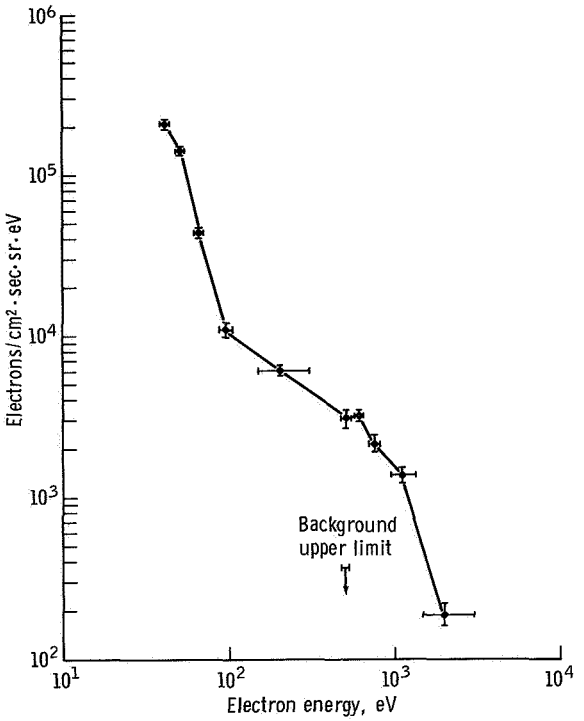

FIGURE 10–20.—Electron energy spectrum measured by analyzer A between 40 and 2000 eV from 21:45 to 22:00 G.m.t., March 10, the period of high, stable flux shown in figure 10–18.

The energy spectrum and total flux of electrons and the temporal history of the event suggest that these data represent an observation of the particles of a thin neutral sheet moving across the site. The difficulty with this interpretation lies in the fact that, at this time, the CPLEE was approximately $6R_E$ away from the theoretical location of the neutral sheet, the Y_{SM} axis (fig. 10–19). Strong indications exist, however, that the solar-magnetospheric coordinate system does not aid in locating the neutral sheet with an error of less than approximately $10R_E$ at lunar distances. The neutral-sheet observations with a magnetometer on board the Interplanetary Monitoring Platform 1 satellite (ref. 10–14) locate the neutral sheet at various times during the period March 22 to May 26, 1964, in the range $-2R_E < Z_{SM} < 5R_E$. Hence, it is plausible that the neutral sheet could have been located at $Z_{SM}=6R_E$ at the time of the CPLEE observation. Further measurements during forthcoming magnetospheric tail passes by the

CPLEE are needed to effect a definite resolution of this question.

Electron Spectra Similar to Auroral Spectra

On several occasions when the CPLEE was in the magnetospheric tail, short-duration electron enhancements in all ranges of the instrument were observed. These enhancements typically had durations of a few minutes. The energy spectrum of one such enhancement at 23:16 G.m.t., February 7, is shown in figure 10–21. As in most electron spectra observed when the lunar surface is illuminated, the spectrum between 40 and 100 eV is dominated by the photoelectron continuum. However, in the higher energy ranges, a double-peak structure with a low-energy peak in the range 300 to 500 eV and a high-energy peak at 5 to 6 keV can be seen. It is interesting to compare these spectra with spectra observed above a terrestrial aurora. A set of spectra observed above an aurora (measured with a SPECS detector on board a Javelin sounding rocket) is shown in figure 10–22 from reference 10–1. (It should be recalled that the basic particle detectors of both the SPECS and the CPLEE are very similar.)

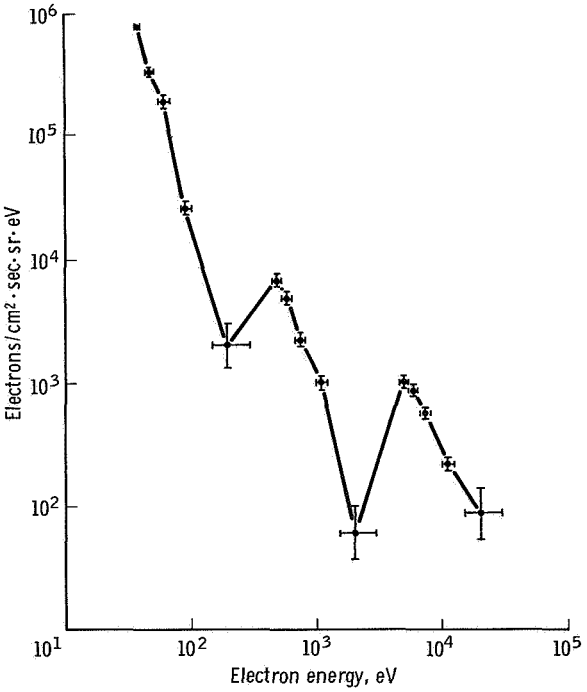

FIGURE 10–21.—Electron energy spectrum of a typical "auroral-electron" event measured by the CPLEE in the magnetospheric tail. Of particular note is the double-peak structure, with a low-energy peak at 300 to 500 eV and a higher energy peak at 5 to 6 keV.

The photoelectron continuum is, of course, absent from these auroral spectra; but, aside from that, a remarkable similarity between the electron fluxes recorded by the CPLEE and the auroral electrons is readily evident. The double-peak structure in both spectra, the low-energy peaks in the 100- to 500-eV range, and the high-energy peaks at 5 to 6 keV are particularly noteworthy. The flux levels in the auroral spectrum are within a factor of 5 of the flux levels measured by the CPLEE (fig. 10–21). Furthermore, while particles measured above an aurora tend to be more or less isotropically distributed about the field lines, the magnetic-tail particles observed by the CPLEE were strongly peaked along the field lines. This deduction was made on the basis of the observation that no flux enhancements were seen in analyzer B, and that the angles between the magnetic field and the directions of analyzers A and B were approximately 20° and 80°, respectively. Particles energized near the Earth and subsequently traveling back into the tail would be sharply peaked along field lines at lunar distances according to the first invariant $\sin^2 \alpha/B = \text{constant}$, where α is the particle pitch angle and B is the local magnetic-field magnitude.

Consequently, the process that produces energetic particles above a terrestrial aurora may well result in the appearance of similar particles in the magnetospheric tail. A definite resolution of this question awaits further study of the data and correlation between the CPLEE data and Earth-based measurements of auroral activity. However, this preliminary indication of auroral particles at large distances from the Earth in the magnetospheric tail implies that some auroral-zone magnetic-field lines are linked with field lines stretching far into the tail and, hence, give information on the general topology of the magnetosphere.

Rapid Temporal Solar-Wind Variations

When the Moon crosses from the magnetospheric-tail regions into interplanetary space on the dawn side of the magnetosphere, the CPLEE analyzer B is pointed toward the Sun and, hence,

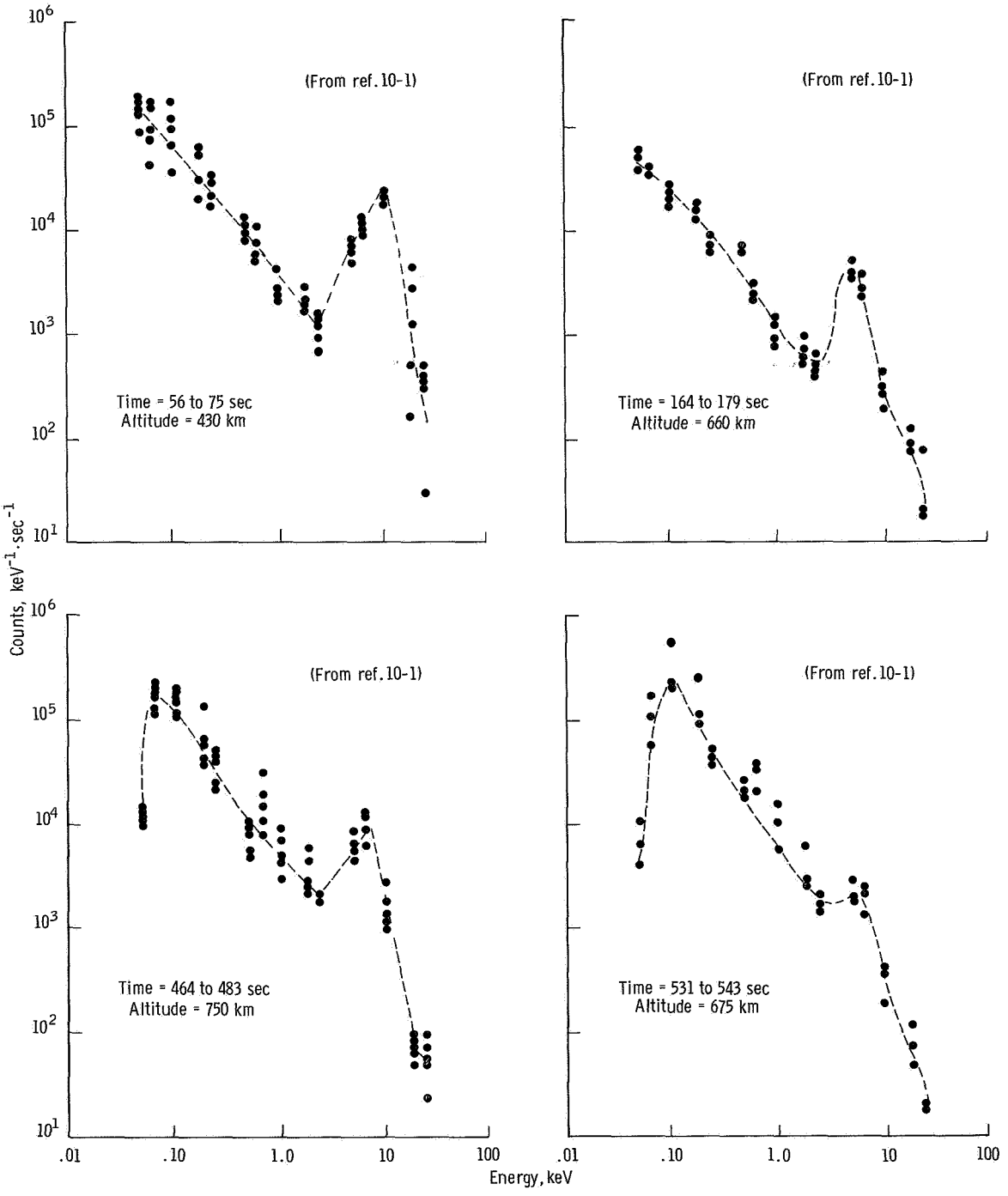

FIGURE 10–22.—Electron spectra measured above a terrestrial aurora by a device similar to the CPLEE on a sounding rocket probe (ref. 10–1). Striking similarities exist between these spectra and the CPLEE magnetospheric-tail electron spectrum shown in figure 10–21.

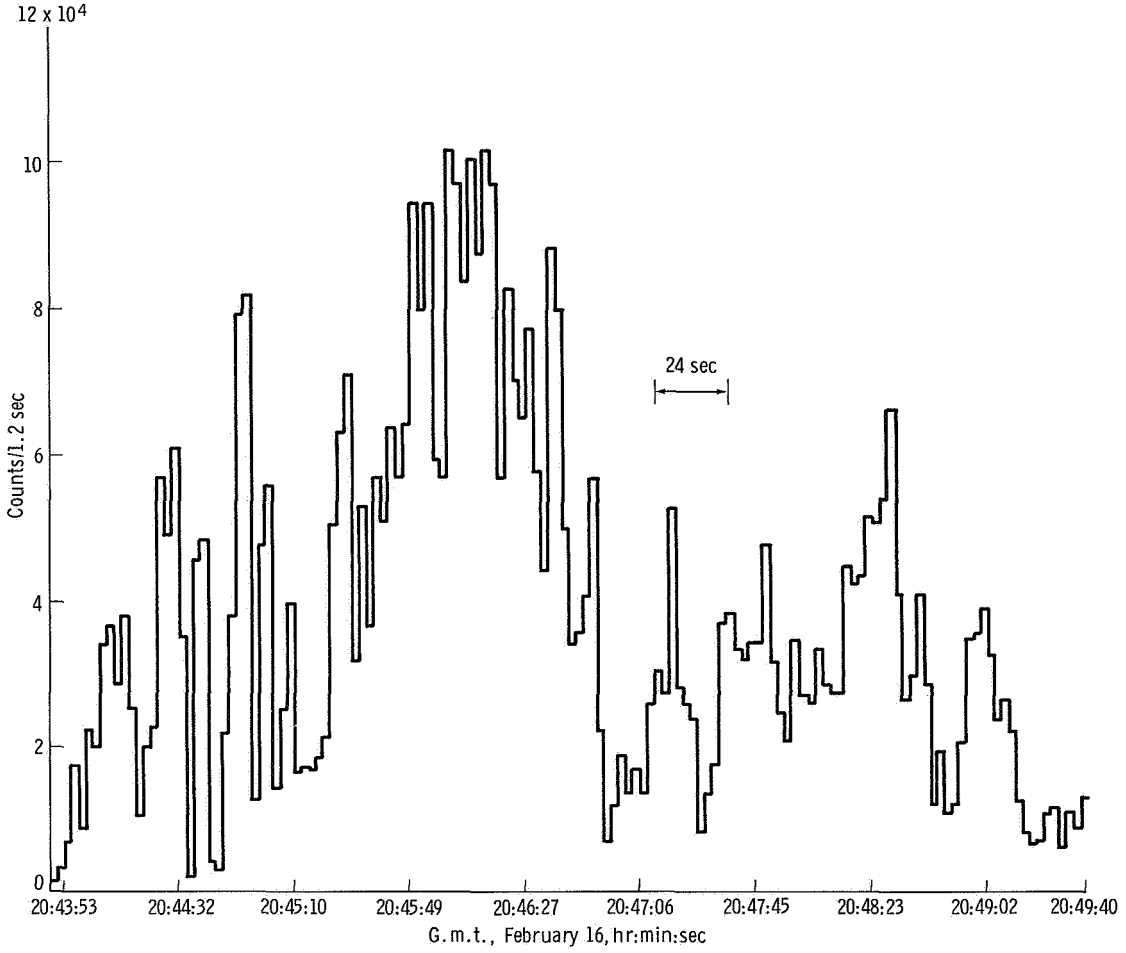

FIGURE 10–23.—An example of rapid temporal variations in solar-wind fluxes. Data from channel 5 of analyzer *B* at 350 V, sensitive to ions with energies between 1.5 and 3 keV, are plotted with a time resolution of 2.4 sec.

is able to detect solar-wind fluxes striking the Moon. Some of the detailed characteristics of solar wind at the lunar surface have been reported previously (ref. 10–4), and the CPLEE measurements appear to be in general agreement with the measurements of average solar-wind parameters by the Apollo 12 solar-wind spectrometer. The unique rapid-sampling capability of the CPLEE has been used to study rapid temporal variations in the solar wind. The sampling interval of the CPLEE (2.4 sec) is compared with those of other experiments designed to measure solar-wind fluxes, notably the Vela 3A and 3B detectors with sampling intervals of 256 sec in reference 10–15 and with the solar-wind spectrometer sampling interval of 28.1 sec in reference 10–4.

An example of rapid solar-wind variations is shown in figure 10–23. At 20:45 G.m.t. on February 16, the solar-magnetospheric coordinates of the CPLEE were $Y_{SM} = -67R_E$ and $Z_{SM} = -32R_E$, placing the instrument well away from the magnetospheric-tail boundary. The angle between the center of the detector field of view and the CPLEE-Sun line was 2°. The CPLEE data showed the counting rate was concentrated in channel 5 at 350-V deflection (the channel sensitive to ions with energies between 1.5 and 3.0 keV, exactly what would be expected if the instrument

were viewing the direct solar wind). The ratio of the counting rates of this channel in analyzer *B* to the corresponding channel in analyzer *A* was on the order of 1000:1, indicating the extreme directionality of the flux.

Variations in the solar-wind flux of up to a factor of 10 on time scales as short as 5 sec are shown in figure 10–23. A comparison of the cyclotron radius of a 1.5-keV proton in the 5γ interplanetary field (1000 km) with the linear velocity of the Moon (1 km/sec) indicates that these variations are indeed temporal in nature. If the variations were spatial in origin, variations in the flux of a factor of 10 over distances as short as 1/200 of a cyclotron radius would be required. This situation is highly unlikely.

An isolated feature of the data has not been selected, and the indication is that these rapid temporal variations are a persistent feature of the solar-wind flux. Lacking a detailed analysis of the frequency spectra of these variations, their origin can only be speculated upon at this time. It is noted, however, that the observed frequency of variations (approximately 0.2 Hz) is similar to the expected observed frequency of magnetoacoustic waves (low-frequency waves that propagate in a magnetized plasma such as the solar wind), the wavelength of which is on the order of an ion-cyclotron radius, as seen by a stationary observer (approximately 0.5 Hz). This suggests that the variations seen are due to magnetoacoustic waves modulating the particle fluxes, and these waves may be generated at the shock surface between the solar wind and the magnetospheric tail.

Summary

During the first month of operation, the CPLEE has detected particle fluxes at the lunar surface resulting from a wide range of lunar-surface, magnetospheric, and interplanetary phenomena. Preliminary data analysis has revealed the presence of a lunar photoelectron layer, an indication of modulation or acceleration of low-energy electrons in the vicinity of the Moon, penetration of auroral particles to lunar distances in the magnetospheric tail, detection of electron fluxes in the magnetospheric tail possibly associated with the neutral sheet, strong modulations of solar-wind fluxes, and the appearance of ions and electrons or negative ions with energies up to 100 eV associated with the LM impact. Many of these discoveries were possible only because of the rapid sampling capability of the CPLEE and its ability to measure particles of both charge signs over a wide energy and dynamic range, coupled with the real-time data display and command capability of the ALSEP.

These preliminary findings have resulted from analysis of "quick-look" hardcopy data. Other phenomena are apparent in the data, but adequate characterization and description must await detailed computer analysis of the 200 measurements/min being returned by the CPLEE.

References

10–1. WESTERLUND, L. H.: Rocket-Borne Observations of the Auroral Electron Energy Spectra and Their Pitch-Angle Distribution. Ph.D. thesis, Rice Univ., 1968.

10–2. O'BRIEN, B. J.: Interrelations of Energetic Charged Particles in the Magnetosphere. Ch. IV of Solar Terrestrial Physics, Newman and King, eds., Academic Press (London), 1967, pp. 169–211.

10–3. LYON, E. F.; BRIDGE, H. S.; AND BINSAK, J. H.: Explorer 35 Plasma Measurements in the Vicinity of the Moon. J. Geophys. Res., vol. 72, no. 23, Dec. 1967, pp. 6113–6117.

10–4. SNYDER, CONWAY W.; CLAY, DOUGLAS R.; AND NEUGEBAUER, MARCIA: The Solar-Wind Spectrometer Experiment. Sec. 5 of the Apollo 12 Preliminary Science Report. NASA SP–235, 1970.

10–5. REASONER, D. L.; EATHER, R. H.; AND O'BRIEN, B. J.: Detection of Alpha Particles in Auroral Phenomena. J. Geophys. Res., vol. 73, no. 13, July 1968, pp. 4185–4198.

10–6. O'BRIEN, B. J.: ABNEY, F.; BURCH, J.; HARRISON, R.; ET AL.: SPECS, A Versatile Space-Qualified Detector of Charged Particles. Rev. Sci. Instrum., vol. 38, no. 8, Aug. 1967, pp. 1058–1068.

10–7. BURCH, JAMES L.: Low-Energy Electron Fluxes at Latitudes Above the Auroral Zone. J. Geophys. Res., vol. 73, no. 11, June 1968, pp. 3585–3591.

10–8. MAEHLUM, BERNT N.: On the High Latitude, Universal Time Controlled F-Layer. J. Atmos. Terr. Phys., vol. 31, no. 1, Jan. 1969, pp. 531–538.

10–9. O'Brien, B. J.; Freden, S.; and Bates, J.: Degradation of Apollo 11 Deployed Instruments Because of Lunar Module Ascent Effects. J. Appl. Phys., vol. 41, no. 11, Oct. 1970, pp. 4538–4541.

10–10. Egidi, A.; Marconero, R.; Pizzella, G.; and Sperli, F.: Channeltron Fatigue and Efficiency For Protons and Electrons. Rev. Sci. Instrum., vol. 40, no. 1, Jan. 1969, pp. 88–91.

10–11. Dyal, P.; Parkin, C. W.; and Sonnet, C. P.: Lunar Surface Magnetometer Experiment. Sec. 4 of Apollo 12 Preliminary Science Report. NASA SP–235, 1970.

10–12. Lehnert, B.: Minimum Temperature and Power Effect of Cosmical Plasmas Interacting With Neutral Gas. Rept. 70–11, Royal Inst. Tech., Div. Plasma Phys., Stockholm, Sweden, 1970.

10–13. Ness, N. F.; Behannon, K. W.; Scearce, C. S.; and Cantarano, S. C.: Early Results From the Magnetic Field Experiment on Lunar Explorer 35. J. Geophys. Res., vol. 72, no. 23, Dec. 1967, pp. 5769–5778.

10–14. Speiser, T. W.; and Ness, N. F.: The Neutral Sheet in The Geomagnetic Tail: Its Motion, Equivalent Currents, and Field Line Connection Through It. J. Geophys. Res., vol. 72, no. 1, Jan. 1967, pp. 131–141.

10–15. Gosling, J. T.; Ashbridge, J. R.; Bame, S. J.; Hundhausen, A. J.; and Strong, I. B.: Satellite Observations of Interplanetary Shock Waves. J. Geophys. Res., vol. 73, no. 1, Jan. 1968, pp. 43–50.

ACKNOWLEDGMENTS

A large number of people contributed to the success of the CPLEE, both directly and indirectly through development of the SPECS and of the calibration equipment. Rice University personnel who made major contributions are Wayne Smith, John Musselwhite, James Ballentyne, John McGarity, David Nystrom, William Porter, Foster Abney, James Burch, and Tad Winiecki.

Bendix personnel who played principal roles were Joe Clayton, Park Curry, Al Robinson, Charles Hocking, William Stanley, George Burton, Lou Paine, Lowell Ferguson, John Ioannau, Jack Dye, Mark Brooks, Charles Flint, and Jerome Pfeiffer.

Numerous NASA personnel played important roles in many phases of the program. Among them must be included Dick Moke, Jack Small, Don Wiseman, Ausley Carraway, J. B. Thomas, and W. K. Stephenson of the NASA Manned Spacecraft Center as well as Dr. J. Naugle, Dr. A. Opp, and E. Davin of NASA Headquarters and A. Spinak of Wallops Station.

This work was supported by NASA contract NAS 9–5884 and analysis was assisted in part by the Science Foundation in Physics at the University of Sydney, Sydney, Australia. Feasibility studies of the CPLEE were supported in part by NASA contracts NAS r–209, NAS 6–1061, and NAS 9–4822.